Available online at www.sciencedirect.com
SCIENCE DIRECT®

Journal of the European Ceramic Society 23 (2003) 91–97
www.elsevier.com/locate/jeurceramsoc

Influence of impurities in Al_2O_3 ceramics on hot corrosion resistance against molten salt

Takehiko Hirata*[,a], Satoshi Ota[b], Tatsuo Morimoto[b]

[a] *Yokohama Research and Development Center, Mitsubishi Heavy Industries, Ltd, 12 Nishiki-cho, Naka-ku, Yokohama, 231-8715 Japan*
[b] *Advanced Technology Research Center, Mitsubishi Heavy Industries, Ltd., 8-1 Sachiura 1-chome,Kanazawa-ku, Yokohama, 236-8515, Japan*

Received 20 September 2001; received in revised form 21 February 2002; accepted 11 March 2002

Abstract

This report describes an investigation of the influence of impurities of Al_2O_3 on the hot corrosion resistance against V_2O_5–Na_2SO_4 molten salt. Thickness of damage zone in Al_2O_3 ceramics whose purity is high depends on the holding time linearly. On the other hand, thickness of damage zone in Al_2O_3 whose purity is relative low depends on square root of holding time. In the impurities, SiO_2 affected the corrosion rate of Al_2O_3 especially. Grain boundaries are suffered from hot corrosion. SiO_2 would influence the diffusion rate of corrosive elements through grain boundaries and the corrosion rate. © 2002 Elsevier Science Ltd. All rights reserved.

Keywords: Al_2O_3; Corrosion resistance; Grain boundaries; Molten salts

1. Introduction

Ceramics have been looked to for future application in hot structural parts of energy plants, which are anticipated to prevent the corrosion attack by molten salts, because they exhibit the superior corrosion resistance against the molten salts.[1] Regarding the corrosion characteristics of ceramics in the molten salt, there are study reports on the corrosion behaviors in sulfate of the non-oxide system ceramics such as Si_3N_4 and SiC, used for gas turbines, etc.[2–4] However, application of the oxide system ceramics having a small effect of oxidation would be adequate in plants using inferior fuels, which provide severe conditions to ceramics used.

Researches on the corrosion behaviors of oxides in the molten salts have principally been conducted on the ZrO_2 ceramics that have an excellent heat resistance and serviceability as the coatings are thermally sprayed.[5–13] Bratton et al.[6] studied the corrosion of Y_2O_3-stabilized ZrO_2 ceramics in the molten salt containing V_2O_5 and concluded that ZrO_2 is de-stabilized due to the formation of YVO_4, resulting in evolution of corrosion. Watanabe et al.[7] conducted a corrosion test of CaO-stabilized ZrO_2 in Na_2SO_4-25 mass% NaCl and clarified that de-stabilization due to formation of $CaSO_4$ causes corrosion. Pettit et al.,[8] also conducted a corrosion test of YSZ in $NaVO_3$ and clarified that a porous layer is formed over the YSZ surface. As shown above, it has already been made clear that corrosion of the ZrO_2 ceramics evolves, caused by its de-stabilization due to the molten salt, and thus, it is needed to find out some oxides with small reactivity from the molten salt, as stabilizing agents for the ZrO_2 ceramics,[14] and to pursue for some oxide ceramics without their phase transitions.

The Al_2O_3 ceramics which can show a high melting point and stabilization without showing phase transition at high temperatures like the ZrO_2 ceramics, has a small solubility particularly in the molten salt and is expected to show an excellent corrosion resistance.[15–18] However, Pettit et al.[8] showed a porous zone was developed at the surface of Al_2O_3 sintered bodies in Na_2SO_4–$NaVO_3$ molten salts. They also showed that the thickness of this zone becomes thick as the concentration of V_2O_5 becomes high in these salts. This porous zone is believed to cause the degradation of strength of Al_2O_3, therefore, it is necessary to minimize the thickness of this porous zone. They indicated that grain boundary suffered from molten salts. Also they

---

* Corresponding author.
E-mail address: takehiko_hirata@d.ydmw.mhi.co.jp (T. Hirata).

0955-2219/02/$ - see front matter
PII: S0955-2219(02)00078-X

showed purity of Al_2O_3 affected corrosion resistance. However, they used a 98% Al_2O_3 specimen as the high purity specimen. Also Yoshiba et al.[10] showed that purity of Al_2O_3 influenced corrosion rate in 85 mass% V_2O_5–15 mass% Na_2SO_4 at 900 °C for 2 h. They examined 99.5% Al_2O_3 and 95% Al_2O_3. They reported corrosion resistance of 99.5% Al_2O_3 was higher than that of 95% Al_2O_3. Recently we can obtain Al_2O_3 specimen whose purity is relative high. We believe that using high purity Al_2O_3 leads to the understanding of the roles of impurities on corrosion in the molten salts.

In this study, the hot corrosion resistance of high purity Al_2O_3 ceramics and Al_2O_3 ceramics, which have a small amount of impurities, were investigated in order to understand the roles of impurities in the Na_2SO_4–V_2O_5 molten salts.

2. Experimental procedures

The raw powders used were Al_2O_3 (UA-5105 Showa-Denko Co., purity, 99.998 mass%; average particle size,

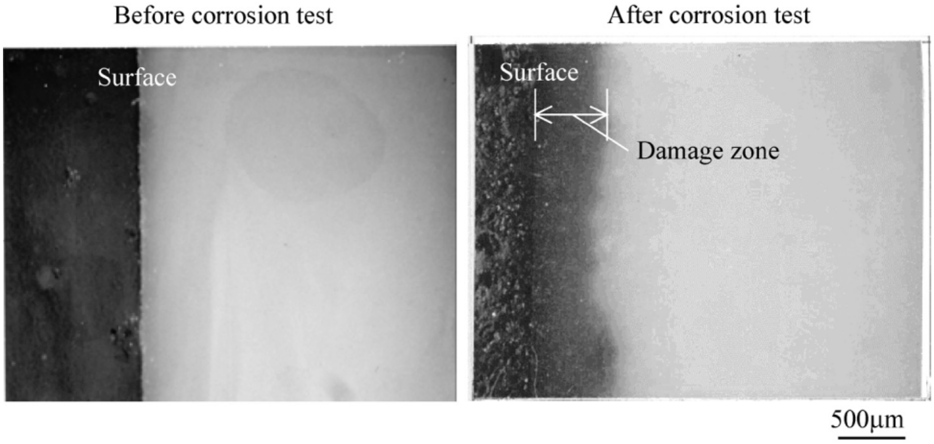

Fig. 1. Cross section of an Al_2O_3 ceramic material before and after corrosion test.

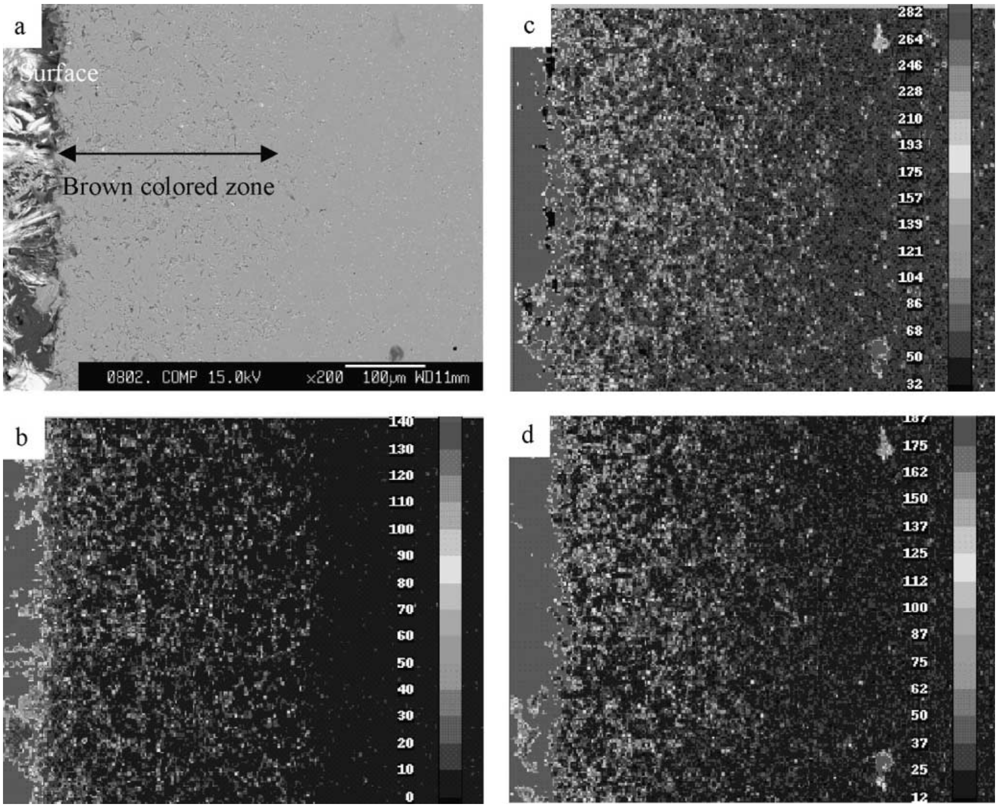

Fig. 2. Microstructure and distribution of elements in the brown colored zone after corrosion test (a) Backscatter image, (b) V map, (c) Na map and (d) S map).

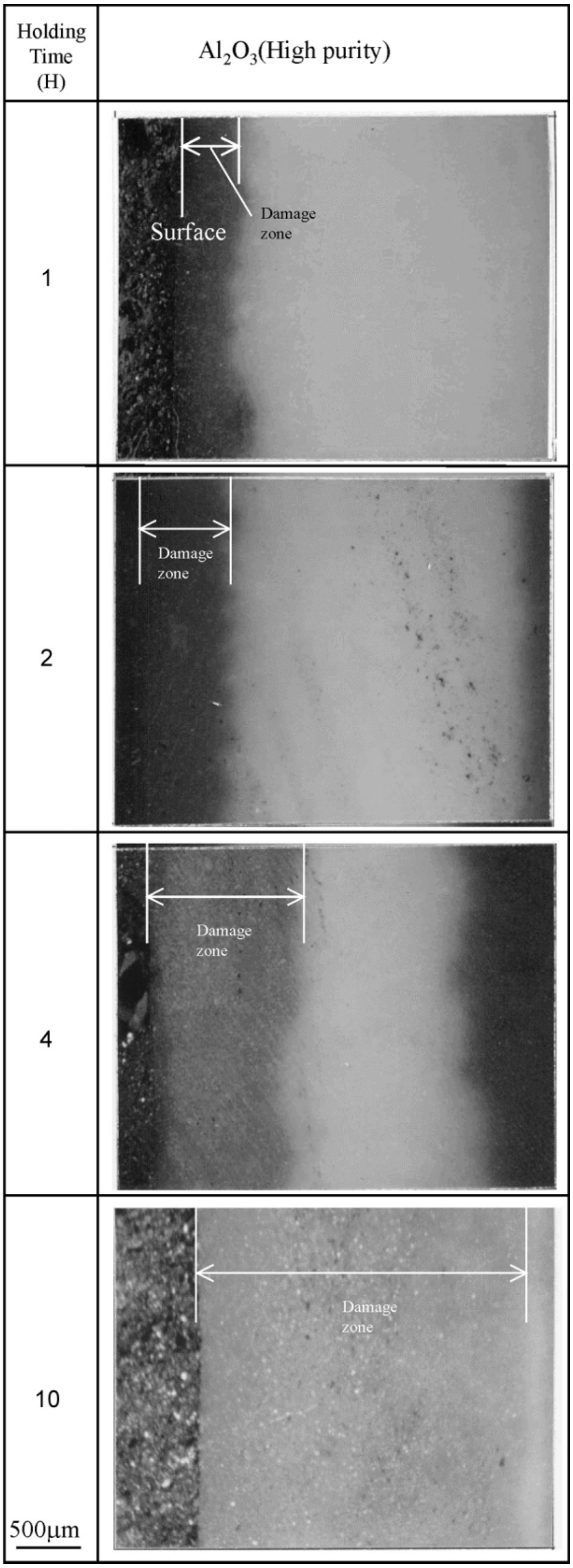

Fig. 3. Cross section of high purity Al_2O_3 at various holding times. (Molten salt: V_2O_5: Na_2SO_4 = 60:40, temperature: 900 °C, atmosphere: air.)

Table 1
Weight change of specimens during corrosion test (temperature: 900 °C, time: 100 h)

Specimen	Weight change (mg/cm^2)
Al_2O_3 (high purity)	3.09
45 mass% Cr–30 mass% Ni–Fe	52.0

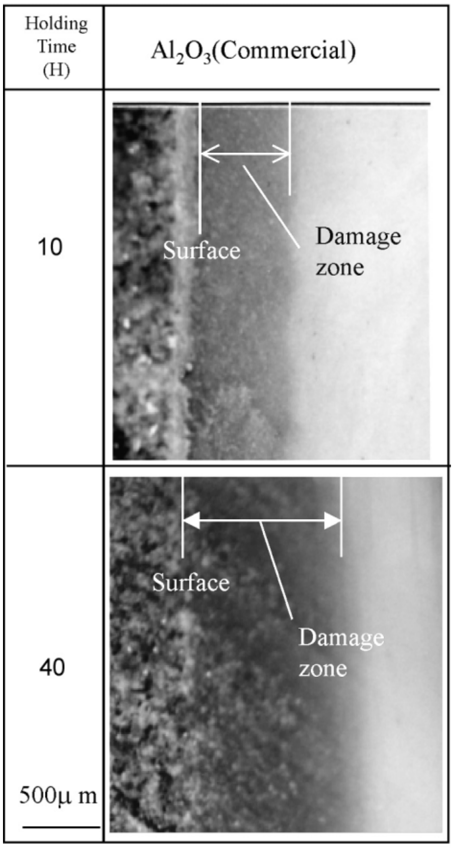

Fig. 4. Cross section of commercial Al_2O_3 at various holding times. (Molten salt: V_2O_5: Na_2SO_4 = 60:40, temperature: 900 °C, atmosphere: air.)

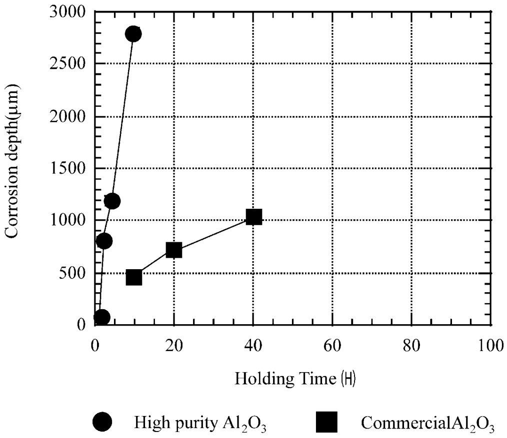

Fig. 5. The relationship between thickness of corrosion damage zone and holding time. (Specimen: high purity Al_2O_3 and commercial Al_2O_3, testing temperature: 900 °C.)

0.2 μm), SiO_2 (Kojyundo Kagaku Co., purity, 99.9 mass%; average particle size, 1 μm), $CaCO_3$ (Kojyundo Kagaku Co., purity, 99.99 mass%) and MgO (MJ-30, Iwatani Kagaku Co., purity, 99.9 mass%; average particle size, 0.5 μm). These powders were mixed in the ethanol with additives for homogeneous mixing of a small amount. Then the powder–ethanol mixture was dried in the oven at a temperature of 80 °C. The derived powder was pressed into disk shapes of about 20 mm in diameter and 5 mm in thickness. Al_2O_3 compacts were sintered at a temperature of 1600 °C for 3 h and 1750 °C for 3 h in an air atmosphere. We also used commercial high purity Al_2O_3 sintered bodies (SSA-S grade purity: 99.71 mass%, Nikkato Co.) in the corrosion test. This sintered body includes 0.1 mass% SiO_2, 0.04 mass% CaO and 0.15 mass% MgO as impurities. The density of sintered bodies was measured from weight and volume of the sintered body. The density of sintered bodies was about 3.98 g/cc which was almost full density.

Hot corrosion tests were carried out in the air atmosphere. The size of the specimen was approximately 15 mm in diameter and 10 mm in height. The surface of the specimens was polished with 1 μm diamond paste. Specimens were poured into crucibles with salts. Crucibles were made of Al_2O_3 whose purities were 99.71%. Salts were composed of 60 mass% V_2O_5 and 40 mass% Na_2SO_4. Crucibles with salts and specimens were heated in the furnace 900 °C for various hours.

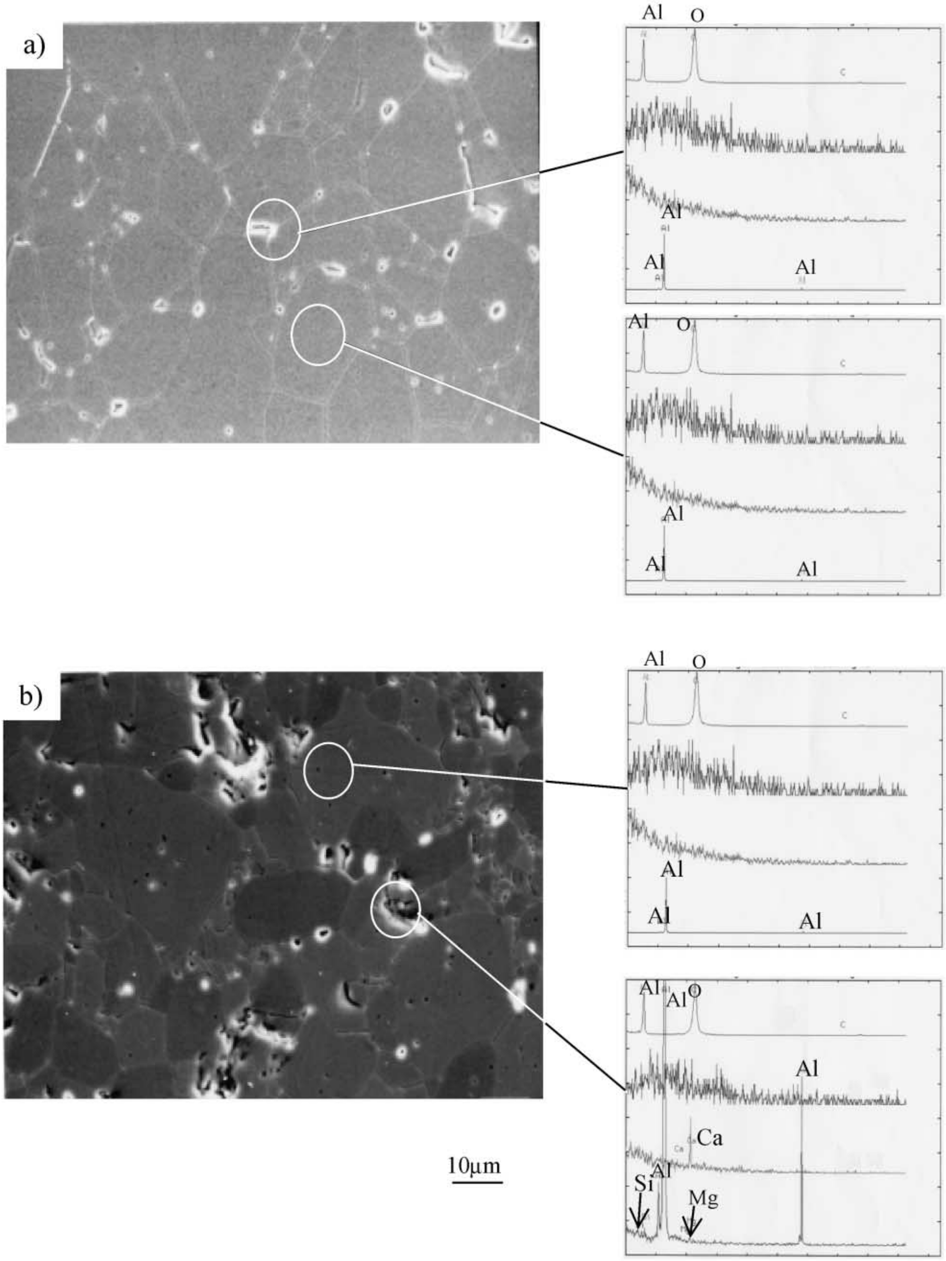

Fig. 6. Microstructure and WDS analysis of Al_2O_3 specimens before corrosion test. (a) high purity Al_2O_3, (b) commercial Al_2O_3.

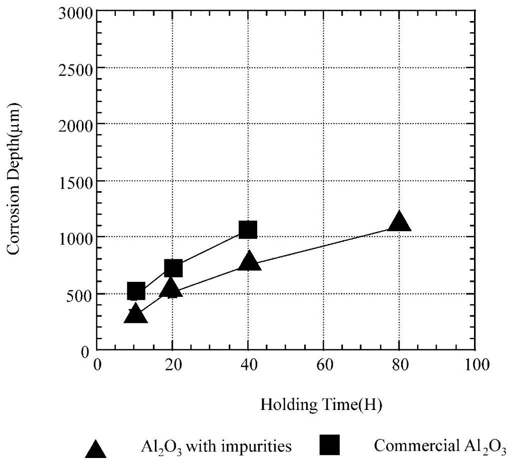

Fig. 7. The relationship between thickness of corrosion damage zone and holding time. (Specimen: high purity Al_2O_3 with the same amount of SiO_2, MgO and CaO as the commercial Al_2O_3 and commercial Al_2O_3, testing temperature: 900 °C.)

Specimens were immersed at the bottom of crucibles during the corrosion test. Specimens were taken out from crucibles and washed in the water of 80 °C for 48 h. Then, weight change after the corrosion test was measured. Also, thickness of the hot corrosion damage zone of the upper surface of the specimens was estimated with an optical microscope.

The microstructure of specimens was observed with the optical microscope (OM, OLYMPUS Co., model VANOX) and the scanning electron microscope (SEM, Jeol Co., model T-33). The distribution of elements of salts was observed with electron probe micro analyzer (EPMA, Jeol Co., model 8864).

3. Results and discussion

Table 1 shows weight change of pure Al_2O_3 and 45 mass% Cr–30 mass% Ni steel as reference during the hot corrosion test for 10 h. Weight change of Al_2O_3 in

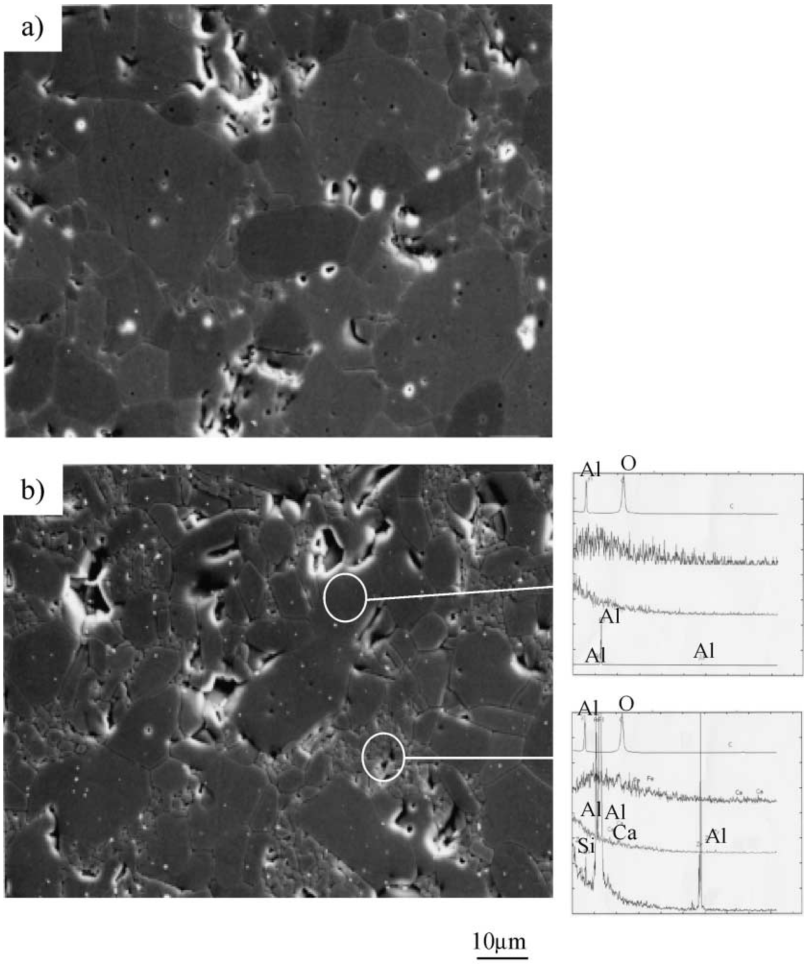

Fig. 8. Microstructure and WDS analysis of Al_2O_3 specimens before corrosion test. (a) commercial Al_2O_3, (b) high purity Al_2O_3 with SiO_2,CaO and MgO.

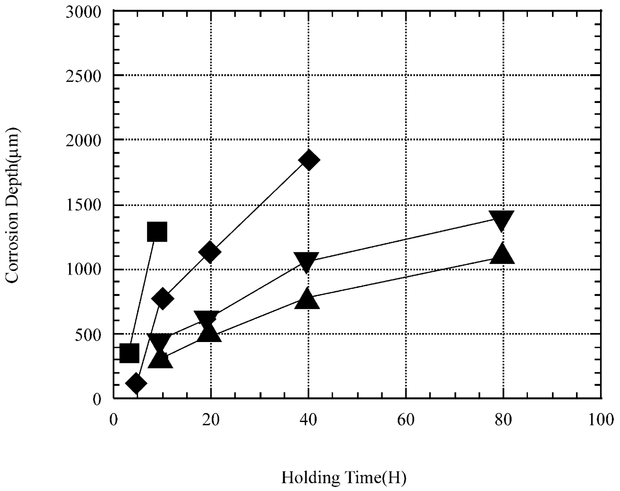

	Contents(mass%)		
	SiO_2	MgO	CaO
▲	0.1	0.15	0.04
▼	0.1	0	0
◆	0	0.15	0
■	0	0	0.04

Fig. 9. The relationship between thickness of corrosion damage zone and holding time. (Specimen: high purity Al_2O_3 with SiO_2, MgO, and CaO, High purity Al_2O_3 with SiO_2, MgO and CaO respectively, testing temperature:900 °C.)

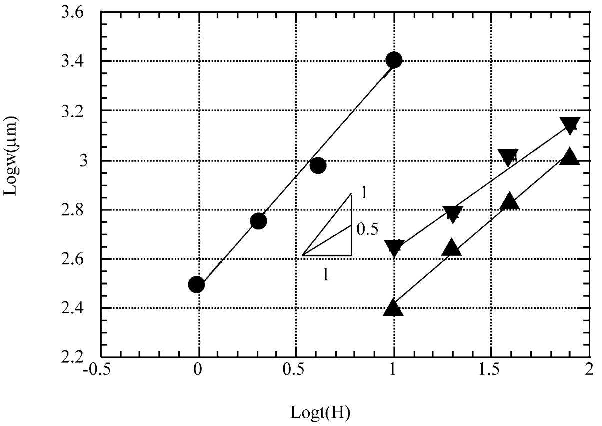

	Contents(mass%)	
	SiO_2	MgO
●	0	0
▲	0.1	0.15
▼	0.1	0

Fig. 10. The relationship between logarithm of thickness of damage zone and holding time. (Specimen: high purity Al_2O_3, Al_2O_3 with SiO_2, Al_2O_3 with SiO_2 and MgO.)

this test is less than that of Cr–Ni steel. A loss of thickness calculated from weight loss is 10 μm or less.

Fig. 1 shows the cross section of high purity Al_2O_3 before and after the corrosion test. The color of the surface of the specimen changes from white to brown. The microstructure of this brown zone is indicated in Fig. 2. In this zone, grain boundaries are observed easily. V and Na are detected in the grain boundaries. Therefore, this brown zone is considered to be the damage zone.

Fig. 3 shows the cross section of high purity Al_2O_3 ceramics at various corrosion times. Thickness of the damage zone increases with increasing holding time. Fig. 4 shows the cross section of commercial Al_2O_3 ceramics at various corrosion times. Thickness of this damage zone is less than that of the high purity Al_2O_3 specimen. This commercial Al_2O_3 specimen includes 0.1 mass% SiO_2 and 0.15 mass% MgO as impurities. Fig. 5 shows the relationship between thickness of the corrosion damage zone and holding time. Corrosion rate of high purity Al_2O_3 is larger than that of commercial Al_2O_3. Thickness of the damage zone of the high purity Al_2O_3 is proportional to the holding time. On the other hand, that of commercial Al_2O_3 is not proportional to the holding time. Therefore the corrosion rate process of high purity Al_2O_3 seems to be different from that of commercial Al_2O_3. Fig. 6 shows microstructures of high purity Al_2O_3 and commercial Al_2O_3 before the corrosion test. The diameter of particles of high purity Al_2O_3 is almost same as that of commercial Al_2O_3. Impurities are detected at the grain boundaries of commercial Al_2O_3, and any impurities are not detected at the grain boundaries of high purity Al_2O_3 at all. From these results, impurities at grain boundaries are considered to influence the corrosion rate of Al_2O_3 in the V_2O_5–Na_2SO_4 molten salt.

The corrosion test on high purity Al_2O_3 with the same amount of SiO_2, MgO and CaO as commercial Al_2O_3 was carried out to clarify the effect of these elements on the corrosion rate. Fig. 7 shows the relationship between the thickness of the damage zone of high purity Al_2O_3, Al_2O_3 with impurities and commercial Al_2O_3. Al_2O_3 with impurities exhibited the same corrosion behavior as the commercial Al_2O_3. Fig. 8 shows microstructures of these Al_2O_3 sintered bodies. Particle diameters of these sintered bodies are almost the same. Al_2O_3 with impurities and commercial Al_2O_3 show Si, Mg and Ca at grain boundaries. Therefore, these elements influence the corrosion rate of Al_2O_3.

The effects of these elements are investigated respectively. Fig. 9 shows the relationship thickness of the damage zone and holding time on Al_2O_3 with SiO_2, MgO and CaO respectively. Fig. 9 also shows the relationship thickness of the damage zone and holding time on Al_2O_3 with all the impurities: SiO_2, MgO and CaO. Al_2O_3 with SiO_2 shows the same corrosion rate as commercial Al_2O_3 and Al_2O_3 with SiO_2, MgO and CaO. Fig. 10 shows the relationship between the logarithm of the thickness of the damage zone and logarithm of the holding time. Corrosion rate of high purity Al_2O_3 is proportional to the holding time. On the other hand, commercial Al_2O_3, Al_2O_3 with SiO_2, MgO and CaO and Al_2O_3 with SiO_2 are proportional to the square root of the holding time. Therefore, the corrosion rate of Al_2O_3 with SiO_2 seems to be controlled by the diffusion through the grain boundaries. Pettit et al.[18] shows that SiO_2 makes silicate glass at grain boundaries. This silicate glass seems to prevent the diffusion of corrosive elements such as V and Na. Therefore the corrosion rate of Al_2O_3 with SiO_2 and commercial Al_2O_3 seems to be reduced.

4. Conclusions

In this work, we examined the influence of impurities of Al_2O_3 on hot corrosion behavior against molten salt. We obtained the following results:

1. Thickness of the damage zone of high purity Al_2O_3 depends on the holding time linearly. On the other hand, that of commercial Al_2O_3 whose purity is relatively low depends on the square root of the holding time.
2. Al_2O_3 sintered bodies that include the same amount of impurities as commercial Al_2O_3 indicate the same dependence on holding time.
3. Al_2O_3 sintered bodies, which include SiO_2 as an impurity also indicate the same dependence on holding time.
4. The rate step of corrosion is diffusion through the grain boundary layer that includes SiO_2.

References

1. Grabke, H. J., *Corrosion of Advanced Ceramics* 1994, pp. 223–234.
2. Jacobson, N. S., Corrosion of silicon-based ceramics in combustion environments. *J. Am. Ceram. Soc.*, 1993, **76**, 3–28.
3. Sato, T. *et al.*, Corrosion and strength degradation of Si_3N_4 and sialons in K_2CO_3 and K_2SO_4 melts. *J. Mater. Sci.*, 1988, **23**, 1405–1410.
4. Say, W. C. and Liu, S. C., Gaseous corrosion mechanisms of silicon carbides in Na_2SO_4 and V_2O_5 environments. *J. Mater. Sci.*, 1996, **31**, 3003–3008.
5. Mckee, D. W. and Siemers, P. A., Resistance of thermal barrier ceramic coating to hot salt corrosion. *Thin Solid Films*, 1980, **73**, 439.
6. Bratton, R. J. and Lau, S. K., Zirconia thermal barrier coatings. In: Proceedings of the International Conference on the Science and Technology of Zirconia, Cleveland. 1981, p. 226.
7. Watanabe, H. and Chigasaki, M., Hot corrosion resistance of stabilized ZrO_2 to a Na_2SO_4–NaCl molten salt. *Yogyo-Kyokai-Shi*, 1984, **92**, 308.
8. Pettit, F. S. et al., Hot corrosion of oxide ceramics. In *Proceedings of the NATO Advanced Research Workshop on Corrosion of Advanced Ceramics*, ed. K. G. Nickel. Kluwer Academic Publishers, 1993, p. 235–248.
9. Jones, R. L., Reaction of vanadium compounds with ceramic oxides. *J. Electrochem. Soc.*, 1986, **133**, 227.
10. Yoshiba, M. *et al.*, V_2O_5–Na_2SO_4–NaCl molten salt corrosion behavior of various high temperature structural ceramics. In *High Temperature Corrosion of Advanced Materials and Protective Coatings*. Elsevier Science Publishers, London, 1992, pp. 355.
11. Harada, Y., et al., Failure analysis of some plasma spray coated superalloy systems subject to the synergistic high temperature damages in actual gas turbine or in laboratory. In *Proceedings of Thermal Spraying, Held at Kobe Japan, May* 1995. High Temperature Society of Japan, 1995, p. 89.
12. Yamamoto, H. *et al.*, Hot corrosion resistance of ZrO_2 ceramics to molten salt. *Mitsubishi Jyuko Giho*, 1988, **25**, 25.
13. Yoshiba, M. *et al.*, High temperature oxidation and hot corrosion behavior of two kinds of thermal barrier coating systems for advanced gas turbines. *J. Thermal Spray Technology*, 1996, **5**, 259.
14. Jones, R. L., Scandia-stabilized zirconia for resistance to molten vanadate-sulfate corrosion. *Surface and Coatings Technology*, 1989, **39/40**, 89.
15. Rapp, R. A., Hot corrosion of materials. In *High-Temperature Chemistry*. Elsevier Science Publishers, 1989, pp. 291–329.
16. Nishida, K. *et al.*, Corrosion resistivity of Ceramics. *Boshoku Gijutsu*, 1986, **35**, 646–666.
17. Yamamoto, H. *et al.*, Hot corrosion resistance of Al_2O_3 ceramics ro molten salt. *Mitsubishi Jyuko Giho*, 1987, **24**, 74.
18. Pettit, F. S. *et al.*, Hot corrosion of Al_2O_3. *J. Mater. Res.*, 1993, **8**, 1964.